

Ultra-diffuse galaxies: the high-spin tail of the abundant dwarf galaxy population

N. C. Amorisco^{1,2*}, A. Loeb¹

¹*Institute for Theory and Computation, Harvard-Smithsonian Center for Astrophysics, 60 Garden St., MS-51, Cambridge, MA 02138, USA*

²*Max Planck Institute for Astrophysics, Karl-Schwarzschild-Strasse 1, D-85740 Garching, Germany*

31 March 2016

ABSTRACT

Recent observations have revealed the existence of an abundant population of faint, low surface brightness (SB) galaxies, which appear to be numerous and ubiquitous in nearby galaxy clusters, including the Virgo, Coma and Fornax clusters. With median stellar masses of dwarf galaxies, these ultra-diffuse galaxies (UDGs) have unexpectedly large sizes, corresponding to a mean SB of $24 \lesssim \langle \mu_e \rangle_r \text{ mag}^{-1} \text{ arcsec}^2 \lesssim 27$ within the effective radius. We show that the UDG population represents the tail of galaxies formed in dwarf-sized haloes with higher-than-average angular momentum. By adopting the standard model of disk formation – in which the size of galaxies is set by the spin of the halo – we recover both the abundance of UDGs as a function of the host cluster mass and the distribution of sizes within the UDG population. According to this model, UDGs are not failed L_* galaxies, but genuine dwarfs, and their low SB is not uniquely connected to the harsh cluster environment. We therefore expect a correspondingly abundant population of UDGs in the field, with likely different morphologies and colours.

Key words: galaxies: dwarf — galaxies: structure — galaxies: formation — galaxies: haloes — galaxies: clusters

1 INTRODUCTION

The existence of faint and extended galaxies in both field and clusters is certainly not a recent discovery (e.g., Impey et al. 1988; Bothun et al. 1991; Turner et al. 1993; Dalcanton et al. 1997a; Caldwell 2006). However, deep and wide field observations of nearby galaxy clusters have only recently first highlighted that this population is both ubiquitous in clusters and perhaps surprisingly numerous. Using the Dragonfly array (Abraham & van Dokkum 2014), van Dokkum et al. (2015a) (vD15) first identified 47 extended, roundish, quiescent galaxies, with central surface brightness (SB) of $\mu_{g,0} = 24 - 26 \text{ mag arcsec}^{-2}$, in imaging data of the Coma cluster. Their projected spatial clustering and the inability of Hubble ACS observations to resolve them into stars suggested that these are actual cluster members. If so, at a distance of approximately 100 Mpc, these galaxies would have a median stellar mass of only $\approx 6 \times 10^7 M_\odot$, but the sizes of L_* galaxies, $r_e = 1.5 - 4.6 \text{ kpc}$. In fact, membership to Coma has been confirmed for one of them with Keck spectroscopy (van Dokkum et al. 2015b), ascertaining the unusual properties of such ultra-diffuse galaxies (UDGs).

Since then, UDGs have been identified in significant

numbers also in the Virgo cluster (Mihos et al. 2015), the Fornax cluster (Muñoz et al. 2015), in 8 other clusters at redshift $z = 0.044 - 0.063$ (van der Burg et al. 2016, vdB16), and the number of detections in Coma have increased by at least an order of magnitude (Koda et al. 2015, K15). However, the nature of their properties has remained elusive so far.

UDGs do not seem to show any clear evidence for tidal stripping. Also, their colours and spatial distributions within the host clusters imply that many of them have not just been accreted, and that they are capable of surviving the strong cluster tides at pericenter. vD15 soon realised that they have to be dark matter dominated systems. In opposition to classical low SB galaxies (e.g., van der Hulst et al. 1993; McGaugh & Bothun 1994; Schombert et al. 2011), UDGs appear quenched, and populate the red sequence. This has brought vD15 and K15 to suggest that their existence could be strictly linked with the cluster environment, and possibly that UDGs might represent ‘failed’ L_* galaxies, prematurely quenched at infall by gas removal.

Measurements of the internal kinematics of UDGs would constrain their true masses and discriminate between different formation pathways, however this is challenging due to their low SB. Very recently, Beasley et al. (2016) have taken advantage of the unusually abundant globular

* E-mail: nicola.amorisco@cfa.harvard.edu

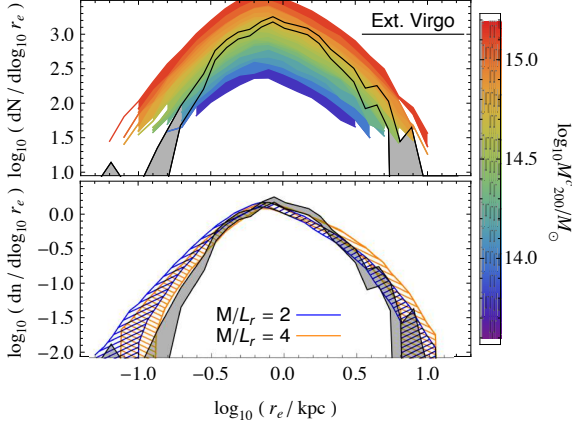


Figure 1. Calibration of our fiducial model against the high SB galaxy population. In both the upper and lower panels, black lines and grey shaded region identify the size distribution of members of the Virgo cluster (Kim et al. 2014). The upper and lower panels compare this with cluster populations obtained from our fiducial model, in terms of absolute galaxy numbers, dN , and relative distributions, $dn = dN/N_{be}$ (N_{be} being the total number of galaxies within the cluster that comply with the cuts that define the Virgo members). Models in the upper panel are colour-coded according to the virial mass of the cluster, M_{200}^c , the hatched regions in the lower panel illustrate the effect of different mass-to-light ratios.

cluster system of VCC 1287, a UDG in the Virgo cluster, and, based on globular cluster spectroscopy inferred a virial mass of only $(8 \pm 4) \times 10^{10} M_{\odot}$. This shows that VCC 1287 is a genuine dwarf galaxy despite its effective radius of 2.4 kpc, disfavoring the possibility of a ‘failed’ L_* galaxy. Interestingly, similar conclusions can be drawn from the hydrodynamical simulations of Yozin & Bekki (2015). These authors show that larger-than-average disk dwarfs infalling onto a cluster are quickly quenched by ram pressure stripping, and reproduce the sizes and colours of many observed UDGs.

In this paper, we show that the properties and abundance of UDGs in clusters are largely compatible with the classical model of disk formation (e.g., Fall & Efstathiou 1980; Dalcanton et al. 1997b; Mo et al. 1998; Dutton et al. 2007). As invoked for classical low SB galaxies (Dalcanton et al. 1997a,b; Mo et al. 1998; Yozin & Bekki 2015), galaxies formed in haloes with a higher initial spin result in larger disks, and therefore, low SB. Here we show that the UDG population discovered so far represents the tail of those dwarf galaxies that formed in haloes with higher-than-average initial angular momentum. Section 2 illustrates our simple model and tests it against the population of normal, high SB galaxies. Section 3 compares the prediction of our fiducial model with the observed properties and abundances of UDGs. Section 4 discusses results and draws conclusions.

2 Λ CDM GALAXY POPULATIONS

We are interested in predicting abundances of galaxies defined by a set of cuts in absolute magnitude, SB and/or galaxy size, within galaxy clusters with mass M_{200}^c . We adopt a very simple model, in which

- The full subhalo population of the cluster is obtained from Monte Carlo generated merger histories, with the spec-

tra of both virial masses and accretion redshifts calibrated on the Millenium simulation (Fakhouri et al. 2010);

- Each of these haloes contains a galaxy with a stellar mass M_* , fixed by a standard abundance matching relation (e.g., Behroozi et al. 2013; Garrison-Kimmel et al. 2014);
- The effective radius of each galaxy is calculated according to the spin parameter of its halo (Mo et al. 1998);
- Galaxies are considered destroyed by $z = 0$ if not compact enough to survive the cluster tidal gravitational field.

We assume that the distribution of halo spin parameters

$$\lambda \equiv J|E|^{1/2}G^{-1}M^{-5/2} \quad (1)$$

is log-normal, with a mean value of $\langle \ln \lambda \rangle = 0.05$ and $\sigma(\ln \lambda) = 0.52$, independent of redshift and halo mass (e.g., Bullock et al. 2001; Vitvitska et al. 2002; Macciò et al. 2007; Kim et al. 2015). The concentration of halos follows the redshift dependent mass-concentration relation compiled by Gao et al. (2008), with a scatter of approximately 0.3 dex (e.g., Ludlow et al. 2014). We adopt the stellar-halo mass relation $M_*(M_{200})$ proposed by Garrison-Kimmel et al. (2014), independently of redshift, with a scatter of 0.3 dex (Behroozi et al. 2013; Mashian et al. 2016). Also, deviations in the properties of each galaxy from the mean relations are assumed to be uncorrelated.

We calculate all effective radii using the model of Mo et al. (1998), with $m_d = j_d = 0.05$, i.e. the specific angular momentum of disks reflects that of their halos, as also supported by observations of star forming galaxies at intermediate redshifts (Burkert et al. 2015). We do not distinguish galaxies according to their morphology, implicitly assuming that the initial spin sets the size of stellar spheroids as it does for disks (Shen et al. 2003; Kravtsov 2013). We use $r_e \equiv R_h$, where R_h is the nominal disk scale-length predicted by the model, as a function of halo mass, concentration, spin parameter, and formation redshift z_f of each galaxy. We calibrate this on average Milky Way-like halos, for which the model predicts $R_h = 3.6$ kpc (as from Bovy & Rix 2013) for $z_f = z_{\min} = 0.7$. Therefore, we take the formation redshift to be the largest between z_{\min} and the infall redshift of each halo onto the cluster.

Our final cluster populations only include galaxies that survive the cluster tides according to the Roche criterion:

$$\frac{M^g(< 2r_e)}{M^c(< r_{\text{peri}})} > 3 \left(\frac{2r_e}{r_{\text{peri}}} \right)^3, \quad (2)$$

where $M^g(< 2r_e)$ is the galaxy mass within twice its effective radius, and $M^c(< r_{\text{peri}})$ is the cluster mass within the orbital pericenter of the galaxy. This is calculated at the accretion redshift, using $r_{\text{peri}} = R_{200}^c/2c$, where R_{200}^c is the virial radius of the cluster at that time and c its concentration, so that the resulting r_{peri} is representative of the common cosmological accretion process (e.g., Benson 2005; Wetzel 2011; Jiang et al. 2015).

We first test the performance of this model on the cluster population of normal, high SB galaxies. We use the Extended Virgo Cluster Catalog (Kim et al. 2014), which collects properties of the 1028 spectroscopic members that comply with the observational cuts

$$\begin{cases} M_r < -13.4 \text{ mag} \\ \langle \mu_e \rangle_r < 24.5 \text{ mag arcsec}^{-2} \end{cases}, \quad (3)$$

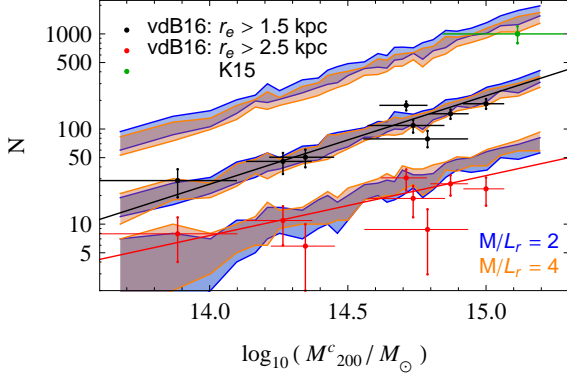


Figure 2. Comparison of predicted UDG abundances N with available measurements, as a function of the cluster virial mass. Data points and fitting lines display measurements from vdB16 and K15. Different colours refer to different defining criteria for the UDG population. Shaded regions extend between the 10 and 90% quantiles for the corresponding populations in our model. Different colours indicate different mass-to-light ratios.

where we indicate the mean SB within the effective radius with $\langle \mu_e \rangle$. In the following, we refer to this population with the term ‘bright end’, so that its abundance in any given cluster is N_{be} . The size distribution of the Virgo galaxies is displayed in Figure 1 using a grey shaded area, and is compared with the predictions of our simple model, that we have used to produce 300 mock clusters, with virial masses M_{200}^c in the interval $13.6 < \log_{10}(M_{200}^c/M_\odot) < 15.3$. The upper panel shows the abundance of the bright end population as a function of the cluster mass. N_{be} depends mildly on the adopted value of the mass-to-light ratio of the population, with $N_{be} = 10^3$ corresponding to a virial mass of $\log_{10}(M_{200}^c/M_\odot) = (14.8 \pm 0.2)$ for galaxies with $M/L_r = (3 \pm 1)M_\odot/L_\odot$, in good agreement with the mass of Virgo within the wide area covered by the Extended Virgo Cluster Catalog (e.g., Fouqué et al. 2001; Côté et al. 2004). The lower panel of Fig. 1 compares the relative distribution of galaxy sizes within the bright end population, which matches well the measured bell-shape.

3 THE UDG POPULATION

The recent work of vdB16 is very useful to test our model, as it presents quantitative criteria defining the observed UDG samples. We apply the same cuts to our cluster galaxy populations and compare the results. First, we address the abundances N of UDGs with the following set of properties

$$\begin{cases} M_r < -13.8 \text{ mag} \\ 24 < \langle \mu_e \rangle_r \text{ mag}^{-1} \text{ arcsec}^2 < 26.5 \\ r_e > 1.5 \text{ kpc} \end{cases}, \quad (4)$$

as used by vdB16 to measure UDG abundances in 8 clusters at redshift $z \approx 0.05$. Black points and the black guiding line display such measurements in Figure 2. The underlying shaded regions cover the area between the 10% and the 90% quantiles as predicted by our model for the same abundances, for two different values of the mass-to-light ratio. The quantitative agreement between model predictions and measurements is very good. Red data points and fitting line

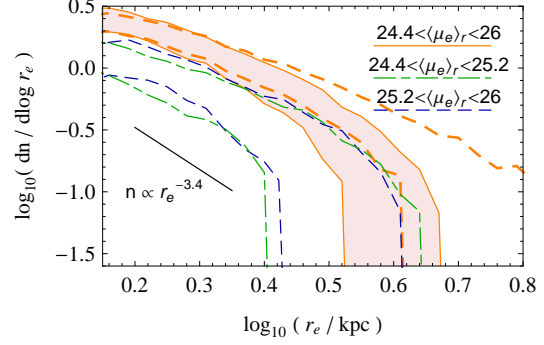


Figure 3. The UDG size distribution. The shaded region shows the size distribution of cluster UDGs, defined as in vdB16, which agrees well with the measured slope $n \propto r_e^{-3.4}$, illustrated by the black guiding line (field UDGs are displayed with an orange dashed profile). The green and blue dashed styles display the size distribution of two subsets of the same UDG population, defined according to SB as in the legend. As measured by vdB16, UDGs are approximately uniform in SB.

are obtained from the same observational dataset, but only include the largest UDGs in the sample, with a more extreme cut of $r_e > 2.5$ kpc. As for the full UDG population, this tail is also quite well reproduced by our model. Finally, Fig. 2 displays, with a green point, the measurement performed by K15 for the abundance of UDGs in the Coma cluster. They adopt the definition

$$\begin{cases} M_r < -12 \text{ mag} \\ 24.3 < \langle \mu_e \rangle_r \text{ mag}^{-1} \text{ arcsec}^2 < 27.3 \\ r_e > 0.8 \text{ kpc} \end{cases}, \quad (5)$$

which samples both fainter and less diffuse systems, therefore reaching an abundance of approximately 1000 UDGs in the cluster. Applying these cuts to our galaxy populations produces similar abundances, as shown by the shaded regions. As the stellar M/L ratio is only weakly variable, we uniformly adopt $M/L_r = 3 M_\odot/L_\odot$ in the following.

vdB16 has measured the size distribution within the UDG population, defined adopting the cuts of eqn (4), but with a more restrictive SB constraint, $24.4 < \langle \mu_e \rangle_r \text{ mag}^{-1} \text{ arcsec}^2 < 26$. They find a steep decline with size, well fit by a power-law relation $n \propto r_e^{-3.4}$. Furthermore, they find that the UDGs are approximately equally split between two equal-size bins in SB. Figure 3 shows the corresponding predictions from our model. We recover both a compatible decline in the size distribution, and the approximate uniformity in SB of the UDGs defined this way. The apparent truncation in the size distribution of our cluster UDG population is due to the criterion (2), which forces all infalling UDGs on the same quite radial orbit; such truncation is absent in the field population.

3.1 Physical properties

Figure 4 puts the properties of UDGs into context. The location of the different galaxy populations (3, 4, 5) is shown in the plane of stellar-halo mass and in the plane of spin parameter against deviation from the mean halo concentration. Contours of different thickness include 50, 90 and 99% of the full populations. We find that UDGs are not failed

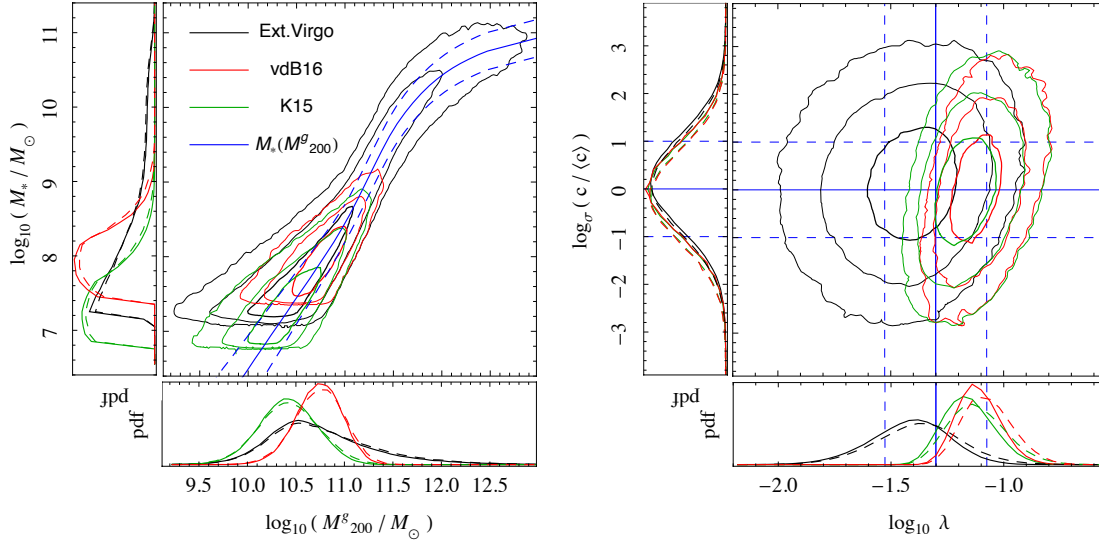


Figure 4. The left and right panels illustrate the location of the UDGs in the plane (M_{200}, M_*) and in the plane of halo spin against normalised deviation in the halo concentration. Contours represent 50, 90 and 99% of galaxies. Blue lines show the adopted abundance matching relation in the left panel and the scatter in both spin and concentration distributions in the right panel. The smaller panels show the one-dimensional (projected) distributions. Full and dashed lines identify the cluster and field populations.

L_* galaxies, but genuine dwarf galaxies, with virial masses that, depending on the adopted observational cut, range in the interval $10^{10} - 10^{11} M_\odot$. These follow from the adopted abundance matching relation, which however remains quite uncertain at the low stellar masses relevant to the UDGs, $10^7 - 10^{8.5} M_\odot$ (e.g., Garrison-Kimmel et al. 2016). UDGs do not seem to diverge from the mean stellar-to-halo mass relation, at least not more than the bright end population is oppositely biased towards systems that are more luminous than average. Their concentrations are also average, with a bias towards less concentrated haloes that is similar but opposite in sign to the bias towards higher concentrations seen in the bright end population. Similarly, we identify only limited differences in the distribution of accretion times, with a tendency for UDGs accreted at higher redshifts to be more easily shredded by the cluster tides, due to the redshift dependence of the halo density contrast (e.g., Amorisco 2015). What clearly distinguishes UDGs and the bright end galaxies are their spin distributions. UDGs are concentrated in the high-spin tail of the halo population, centered approximately one sigma away from the mean. The bright galaxies are also biased, but by a much smaller amount and, of course, in the opposite direction.

Dashed profiles in the one-dimensional insets show the distribution of the different populations when the galaxies excised according to requirement (2) are reincorporated. Under the reasonable assumption that the population of haloes infalling onto clusters have a similar mass distribution compared to those that remain isolated, these profiles can be considered representative of the corresponding galaxy populations in a field environment. Field and cluster populations do not display significant differences in their mean physical properties, apart from the tendency of field populations to shift slightly towards higher spin parameters (and therefore larger sizes), illustrating the fact that, according to our model, the most diffuse UDGs are indeed shredded by tides when infalling onto clusters.

4 DISCUSSION

We have shown that the unexpectedly large size and low SB of UDGs are reproduced naturally within the same standard framework that describes the properties of normal high SB galaxies. The combination of a Λ CDM population of haloes and a classical abundance matching relation is sufficient to reproduce the significant numbers of UDGs observed in galaxy clusters, as a result of the extremely abundant population of dwarf galaxies and the sharp decline in the $M_*(M_{200})$ relation at low masses. UDGs are not a different or peculiar new population of galaxies, but rather the natural extension of normal dwarfs into the low SB regime, characterised by high-spin haloes.

According to our simple criterion for survival against the tides, several UDGs are indeed not compact enough, confirming that a cluster environment is a harsh one for these tenuous dwarfs and suggesting that a fraction of the observed UDGs may in fact be on the verge of tidal disruption. Indeed, as noticed by K15, the morphological properties of the observed UDGs are incompatible with them being a population of disks, and their transformation from very extended disks to thin spheroids may well be caused by the interaction with the cluster, through ram pressure stripping and tidal stirring (e.g., Mayer et al. 2001; Kazantzidis et al. 2011).

However, the cluster itself is not strictly necessary for the formation of dwarf galaxies with such a low SB. Under the assumption that the spin distribution is not strongly dependent on environment (e.g., Macciò et al. 2007; Kim et al. 2015) and that these extended disks are capable of forming stars in a similar way when in isolation, our model suggests that an abundant tail of extended galaxies should be ubiquitous in both clusters and in the field. In fact, Martinez-Delgado et al. (2016) have recently discovered a UDG, DGSAT I, in the outskirts of the Pisces-Perseus supercluster, in a considerably less dense environ-

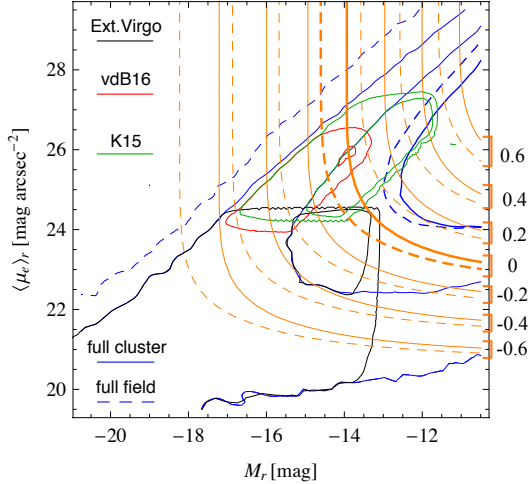


Figure 5. The number density of galaxies in the plane $(M_r, \langle \mu_e \rangle_r)$, relative to the number in the bright cluster population, N_{be} . Colour-coding is as in Fig. 4, with blue contours representing the full galaxy population. The contour sets identify the density values $\{10^{-2.2}, 10^{-1.2}, 10^{-0.6}\}$. Orange contours show the quantity $\log_{10} [N(M_r, \langle \mu_e \rangle_r) / N_{be}]$, where $N(M_r, \langle \mu_e \rangle_r)$ is the total number of galaxies brighter than M_r and with SB higher than $\langle \mu_e \rangle_r$. Full and dashed profiles (in both blue and orange) refer respectively to the cluster and field populations.

ment than the other known UDGs. DGSAT I displays an out-of-center, bluer over-density, compatible with a clump of recently formed stars, and suggesting that the isolated counterparts of cluster UDGs may have more clearly disk morphologies, and not appear as red and quenched. After this manuscript was submitted Roman & Trujillo (2016) reported the detection of a numerous population of UDGs in the large scale structure surrounding the cluster Abel 168, confirming that UDGs can indeed form outside clusters. In support of our model, the same authors also find that the spatial distribution of UDGs is almost identical to that of normal dwarf galaxies, while it is significantly different from the one of L_* galaxies.

Finally, to facilitate comparisons with future observations, Figure 5 provides predictions for the abundance of galaxy populations as a function of the defining cuts, relative to the cluster population in the bright end, N_{be} . Orange lines display contours of the quantity

$$\log_{10} n_{(M_r, \langle \mu_e \rangle_r)} = \log N_{(M_r, \langle \mu_e \rangle_r)} - \log N_{(-13.4, 24.5)} \quad (6)$$

where $N_{(M_r, \langle \mu_e \rangle_r)}$ is the number of galaxies brighter than M_r and with SB higher than $\langle \mu_e \rangle_r$, so that $N_{(-13.4, 24.5)} = N_{be}$. Full and dashed lines refer to the cluster and, even more numerous, field populations.

Our simple model does not directly address the detailed evolutionary pathways of UDGs, how such thin galaxies can indeed form stars, or whether they are made even more dark matter dominated when in a cluster environment with respect to the field. Follow up spectroscopic studies and perhaps the observation of field UDGs will allow better constraints on these issues.

ACKNOWLEDGMENTS

This work was supported in part by NSF grant AST-1312034 (for A.L.).

REFERENCES

- Abraham, R. G., & van Dokkum, P. G. 2014, *PASP*, 126, 55
- Amorisco, N. C. 2015, arXiv:1511.08806
- Beasley, M. A., Romanowsky, A. J., Pota, V., et al. 2016, arXiv:1602.04002
- Behroozi, P. S., Wechsler, R. H., & Conroy, C. 2013, *ApJ*, 770, 57
- Benson, A. J. 2005, *MNRAS*, 358, 551
- Bothun, G. D., Impey, C. D., & Malin, D. F. 1991, *ApJ*, 376, 404
- Bovy, J., & Rix, H.-W. 2013, *ApJ*, 779, 115
- Bullock, J. S., Kolatt, T. S., Sigad, Y., et al. 2001, *MNRAS*, 321, 559
- Burkert, A., Förster Schreiber, N. M., Genzel, R., et al. 2015, arXiv:1510.03262
- Dalcanton, J. J., Spergel, D. N., & Summers, F. J. 1997, *ApJ*, 482, 659
- Dalcanton, J. J., Spergel, D. N., Gunn, J. E., Schmidt, M., & Schneider, D. P. 1997, *AJ*, 114, 635
- Caldwell, N. 2006, *ApJ*, 651, 822
- Côté, P., Blakeslee, J. P., Ferrarese, L., et al. 2004, *ApJS*, 153, 223
- Dutton, A. A., van den Bosch, F. C., Dekel, A., & Courteau, S. 2007, *ApJ*, 654, 27
- Fakhouri, O., Ma, C.-P., & Boylan-Kolchin, M. 2010, *MNRAS*, 406, 2267
- Fall, S. M., & Efstathiou, G. 1980, *MNRAS*, 193, 189
- Fouqué, P., Solanes, J. M., Sanchis, T., & Balkowski, C. 2001, *AA*, 375, 770
- Garrison-Kimmel, S., Boylan-Kolchin, M., Bullock, J. S., & Lee, K. 2014, *MNRAS*, 438, 2578
- Garrison-Kimmel, S., Bullock, J. S., Boylan-Kolchin, M., & Bardwell, E. 2016, arXiv:1603.04855
- Gao, L., Navarro, J. F., Cole, S., et al. 2008, *MNRAS*, 387, 536
- Impey, C., Bothun, G., & Malin, D. 1988, *ApJ*, 330, 634
- Jiang, L., Cole, S., Sawala, T., & Frenk, C. S. 2015, *MNRAS*, 448, 1674
- Kazantzidis, S., Lokas, E. L., Callegari, S., Mayer, L., & Moustakas, L. A. 2011, *ApJ*, 726, 98
- Kim, S., Rey, S.-C., Jerjen, H., et al. 2014, *ApJS*, 215, 22
- Kim, J., Choi, Y.-Y., Kim, S. S., & Lee, J.-E. 2015, *ApJS*, 220, 4
- Koda, J., Yagi, M., Yamanoi, H., & Komiyama, Y. 2015, *ApJL*, 807, L2
- Kravtsov, A. V. 2013, *ApJL*, 764, L31
- Ludlow, A. D., Navarro, J. F., Angulo, R. E., et al. 2014, *MNRAS*, 441, 378
- Macciò, A. V., Dutton, A. A., van den Bosch, F. C., et al. 2007, *MNRAS*, 378, 55
- Martinez-Delgado, D., Laesker, R., Sharina, M., et al. 2016, arXiv:1601.06960
- Mashian, N., Oesch, P. A., & Loeb, A. 2016, *MNRAS*, 455, 2101

- Mayer, L., Governato, F., Colpi, M., et al. 2001, *ApJ*, 559, 754
- McGaugh, S. S., & Bothun, G. D. 1994, *AJ*, 107, 530
- Mihos, J. C., Durrell, P. R., Ferrarese, L., et al. 2015, *ApJL*, 809, L21
- Mo, H. J., Mao, S., & White, S. D. M. 1998, *MNRAS*, 295, 319
- Muñoz, R. P., Eigenthaler, P., Puzia, T. H., et al. 2015, *ApJL*, 813, L15
- Praton, E. A., & Schneider, S. E. 1994, *ApJ*, 422, 46
- Roman, J., & Trujillo, I. 2016, *arXiv:1603.03494*
- Schombert, J., Maciel, T., & McGaugh, S. 2011, *Advances in Astronomy*, 2011, 143698
- Shen, S., Mo, H. J., White, S. D. M., et al. 2003, *MNRAS*, 343, 978
- Turner, J. A., Phillipps, S., Davies, J. I., & Disney, M. J. 1993, *MNRAS*, 261, 39
- van der Burg, R. F. J., Muzzin, A., & Hoekstra, H. 2016, *arXiv:1602.00002*
- van der Hulst, J. M., Skillman, E. D., Smith, T. R., et al. 1993, *AJ*, 106, 548
- van Dokkum, P. G., Abraham, R., Merritt, A., et al. 2015, *ApJL*, 798, L45
- van Dokkum, P. G., Romanowsky, A. J., Abraham, R., et al. 2015, *ApJL*, 804, L26
- Vitvitska, M., Klypin, A. A., Kravtsov, A. V., et al. 2002, *ApJ*, 581, 799
- Yozin, C., & Bekki, K. 2015, *MNRAS*, 452, 937
- Wetzel, A. R. 2011, *MNRAS*, 412, 49